Analytical and Bioanalytical Chemistry
https://doi.org/10.1007/s00216-019-01986-w

RESEARCH PAPER

An electrochemiluminescence biosensor for the detection of soybean agglutinin based on carboxylated graphitic carbon nitride as luminophore

Cong Zhang[1] · Fangxin Hu[2] · Han Zhang[1] · Shihong Chen[1] · Ruo Yuan[1]

Received: 27 April 2019 / Revised: 6 June 2019 / Accepted: 17 June 2019

Abstract

As an important glycoprotein of the lectin family, soybean agglutinin (SBA) is an anti-nutritional factor with considerable toxic and side effects and plays a significant role in tumor analysis. In order to achieve the sensitive detection of SBA, a sandwich-structured electrochemiluminescence (ECL) biosensor was constructed using carboxylated carbon nitride (C-g-C_3N_4) as luminophore and D-galactosamine (galM) as a recognition element. A glassy carbon electrode (GCE) was modified with Au nanoparticles (Au NPs) for capturing the galM via Au-N bond, and further capturing the target SBA by specific recognition between galM and SBA. In the presence of SBA, the composite C-g-C_3N_4-galM was immobilized onto the electrode. With the increase in the concentration of SBA, the ECL signal from C-g-C_3N_4 increased, thus achieving a signal-on detection of SBA. The linear range of the biosensor was 1.0 ng/mL~10 μg/mL and detection limit for SBA was as low as 0.33 ng/mL. In this construction strategy, C-g-C_3N_4 not only acted as an excellent signal probe, but also as an immobilization matrix to easily achieve a high loading of the small molecule recognition element galM. This strategy provides a simple alternative SBA detection platform.

Keywords Electrochemiluminescence · Carboxylated carbon nitride · Soybean agglutinin · Glycoprotein

Introduction

Electrochemiluminescence (ECL) is a technique that produces chemiluminescence by electrochemical induction [1]. With a high sensitivity, rapid determination, low cost, and simple instrument, ECL has been widely used for immunoassay, nucleic acid, food, and water testing [2–5]. For instance, Yang et al. used CdTe QDs as signal probes to construct an ECL immunosensor for detecting cardiac troponin-I antigen [6]. Li et al. constructed a resonance energy transfer ECL biosensor for detecting microRNA based on Ru $(dcbpy)_3^{2+}$ and CdSe@ZnS QDs [7].

As a semiconductor material, graphitic carbon nitride (g-C_3N_4) not only exhibits an excellent ECL performance but also exhibits many advantages such as non-toxicity, simple synthesis, low preparation cost, good water dispersibility, good biocompatibility, good thermal stability, and chemical stability, thus has been widely researched and used in ECL field [8, 9]. Due to the lack of special functional groups, g-C_3N_4 is commonly functionalized with other nanomaterials such as nobel metal nanomaterial or carbon nanomaterial, to achieve the immobilization of biological molecules [10, 11]. Compared to the above functionalization methods, the carboxylation of g-C_3N_4 is a desirable approach. Introduced carboxyl functional groups make the application of g-C_3N_4 in the sensing field more convenient. The carboxylated g-C_3N_4 (C-g-C_3N_4) can easily crosslink with amino groups of proteins and amino modified nucleic acids. Thus, C-g-C_3N_4, as an excellent ECL luminophores, as well an excellent carrier matrix for proteins and nucleic acids, would greatly expand the application of g-C_3N_4 in ECL sensing.

Lectins, as a group of proteins, are widely present in plants and have been extensively studied because of their abundant biological functions. For instance, lectins exhibit carbohydrate

✉ Shihong Chen
cshong@swu.edu.cn

[1] Key Laboratory of Luminescence and Real-Time Analytical Chemistry (Southwest University), Ministry of Education, College of Chemistry and Chemical Engineering, Southwest University, Chongqing 400715, China

[2] Institute of Materials Science & Devices, Suzhou University of Science and Technology, Suzhou 215009, China

Published online: 06 July 2019

specificities that can be widely used for many purposes, such as cell separation, separation and analysis of composite carbohydrates, and cell surface structure research [12, 13]. Soybean agglutinin (SBA), belonging to lectins group, is a protein from soybean plants. SBA can specifically binds galactose or N-acetylgalactosamine [14] and was often used to analyze cell surface structure [15]. In addition, SBA is an anti-nutritional factor with considerable toxic and side effects and can affect intestinal health by affecting intestinal flora, mucosal immune system, barrier function, and intestinal structure. The toxic and side effects of SBA usually lead to slow growth of the animal, hindering the digestion and absorption of nutrients. Therefore, the accurate determination of SBA is of great significance. Electrochemical methods [16] and enzyme linked immunosorbent assay [17] have been established for detecting SBA. However, the sensitivity of these methods is not satisfactory, so it is meaningful to establish a new method to achieve a high sensitive and rapid detection of SBA.

ECL sensors, as a highly sensitive analytical technique, had attracted increasing attention in the detection of lectins. Currently, the reported ECL sensors for lectins are mainly aimed at concanavalin A (Con A) [18, 19], and the ECL measurement of SBA is rarely reported. For Con A, there is a variety of recognition elements, including glucose oxidase (GOx), horseradish peroxidase (HRP), and phenoxy dextran (Dex). Based on the strong adsorption of nanomaterials for proteins or the π–π stacking between nanomaterials and DexP, the immobilization of those recognition elements can be easily achieved, which made Con A sensors easy be built [20, 21]. However, galactose or N-acetylgalactosamine, as the identification element of the SBA, is a small molecule substance and it is difficult to achieve their immobilization on the electrodes, thus limiting the ECL detection of SBA. So it is meaningful to explore an effective and simple strategy for immobilizing the identification element of the SBA, thus achieving the sensitive detection of SBA.

Herein, a sandwich-structured ECL biosensor was developed using C-g-C_3N_4 as luminophore for detecting SBA. The galactosamine (galM) served as the recognition element of SBA and was directly covalently crosslinked onto the C-g-C_3N_4 through the interaction between the amino groups of galM and the carboxyl groups of C-g-C_3N_4 without introducing other nanomaterials. The Au nanoparticles (Au NPs) immobilized onto the electrode acted as the matrix for capturing the galM and further capturing the target SBA. In the presence of SBA, the obtained C-g-C_3N_4-galM was loaded onto the electrode. The ECL signal from C-g-C_3N_4 increased with the increase in the concentration of target SBA. Due to the excellent ECL performance of C-g-C_3N_4, the constructed biosensor achieved a highly sensitive detection of SBA. Here, C-g-C_3N_4 not only acted as an excellent signal probe but also was an ideal immobilization matrix for high loading of a biological molecule containing the amino groups. C-g-C_3N_4 with abundant carboxyl groups provides an alternative platform for ECL detection of SBA.

Experimental

Reagents and chemicals

Cetyltrimethylammonium bromide (CTAB) and ascorbic acid (AA) were obtained from KeLong Chemical Reagent Co. (Chengdu, China). Aladdin Ltd. (Shanghai, China) provided melamine, glucose, and sodium borohydride ($NaBH_4$). J&K Scientific Ltd. (Beijing, China) provided N-hydroxysuccinimide (NHS), N-(3-dimethylaminopropyl)-N′-ethylcarbodiimidehydrochloride (EDC), and D-galactosamine hydrochloride (galM). Bovine serum albumin (BSA), soybean agglutinin (SBA), triethylamine (Et_3N, 99%), and $HAuCl_4{\cdot}4H_2O$ were provided by Sigma Chemical Co. (St. Louis, MO, USA). The human serum samples were obtained from the 9th People's Hospital of Chongqing and its Committee approved this study. All volunteers gave informed consent.

Apparatus

The MPI-E electrochemiluminescence analyzer from Xi'an Remax Electronic Science & Technology Co. Ltd. (China) and CHI 760E electrochemical work station from Shanghai CH Instruments Co. (China) were used to perform the ECL and cyclic voltammetry (CV) detection, respectively. Platinum wire and modified glassy carbon electrode (GCE) were used as the auxiliary and working electrode, respectively. For the ECL detection and the cyclic voltammetry (CV) detection, the reference electrode Ag/AgCl (sat. KCl) and saturated calomel electrode (SCE) were used, respectively. The UV-2450 spectrophotometer from Shimadzu (Japan) was used to collect the UV–vis absorption spectra in a quartz cuvette (path length 1 cm). The wavelength ranged from 200 to 800 nm. The morphologies of nanocomposites were observed using scanning electron microscopy (SEM, S-4800) with an acceleration voltage of 15–20 kV.

Preparation of C-g-C_3N_4

Firstly, g-C_3N_4 was prepared according to the previously reported one-step calcination method [22]. Melamine (10 g) was added into a ceramic crucible, which was placed in the muffle furnace and heated at 600 °C for 2 h. When cooling to room temperature, g-C_3N_4 was obtained. Then, 1 g of g-C_3N_4 and 100 mL of HNO_3 (5 M) were added into a round bottom flask, and the mixture was refluxed at 125 °C for 24 h. The resulting product was carboxylated carbon nitride (C-g-C_3N_4), which was centrifuged and washed with deionized water until the pH reached 7.0. The collected C-g-C_3N_4 was dispersed in 20 mL deionized water for further use.

Preparation of C-g-C_3N_4-galM

The preparation procedure of C-g-C_3N_4-galM is described in Scheme 1. Firstly, to activate the carboxyl group of C-g-C_3N_4, 100 μL of the mixture containing 40 mM EDC and 10 mM NHS was added into 0.1 mL of C-g-C_3N_4 suspension and the resulting mixture was stirred for 2 h. Subsequently, 500 μL of galM (20 mg/mL) was added into above mixture and the resultant solution was stirred for 8 h. Next, 100 μL of 1% bovine serum albumin (BSA) was added into the above mixture with stirring for 1 h. The C-g-C_3N_4-galM/BSA was centrifuged and washed with distilled water. The collected C-g-C_3N_4-galM/BSA was redispersed in 1 mL deionized water for further use.

Preparation of Au NPs

The Au nanoparticles (Au NPs) were synthesized using a seed-growth method [23]. Firstly, 600 μL of 10 mM ice-cooled $NaBH_4$ aqueous solution was added into a 7.8 mL aqueous solution containing 100 mM CTAB and 0.25 mM $HAuCl_4$. The resultant brownish solution was kept undisturbed at 37 °C for 60 min to completely decompose the remaining $NaBH_4$ in the solution. As a result, a seed solution was obtained. Next, a growth solution was prepared by mixing 31.2 mL of deionized water, 0.8 mL of 10 mM $HAuCl_4$, and 6.4 mL of 100 mM CTAB. Then, 3.8 mL of 0.10 M AA solution was added into the growth solution. Subsequently, 20 μL of the above seed solution was diluted 10 times and was added into the above mixture. The resulting solution was slowly inverted for 10 s and stayed overnight. The resultant Au NPs were centrifuged and washed for three times, and then redispersed in deionized water for further use.

Preparation of the biosensor

Firstly, the GCE with 4-mm diameter was polished using 0.3 μm and 0.5 μm alumina powders, respectively, and followed by rinsing with deionized water and ethanol in turn. Then, 10 μL of Au NPs suspension was dropped onto the treated GCE surface and allowed to dry at room temperature. The obtained AuNPs/GCE was incubated with 10 μL of galM (20 mg/mL) overnight. After immersion cleaning, the modified electrode was incubated with 10 μL of 1% BSA for 30 min to block the non-specific site of Au NPs. As a result, the biosensor (BSA/galM/AuNPs/GCE) was obtained.

Measurement procedure

In order to detect target SBA, the biosensor (BSA/galM/AuNPs/GCE) was incubated with 10 μL of SBA with different concentrations for 60 min and further incubated with 10 μL of C-g-C_3N_4-galM/BSA composite for 60 min. After that, the unbound C-g-C_3N_4-galM/BSA was removed by immersion cleaning. Subsequently, the modified electrode was monitored using MPI-E ECL analyzer with a voltage of 800 V for photomultiplier tube (PMT) and a potential scanning range of 0–2.0 V.

Results and discussion

Characterization of different nanomaterials

The microscopic morphology of nanomaterials was investigated by SEM. Figure 1A displays the SEM image of C-g-

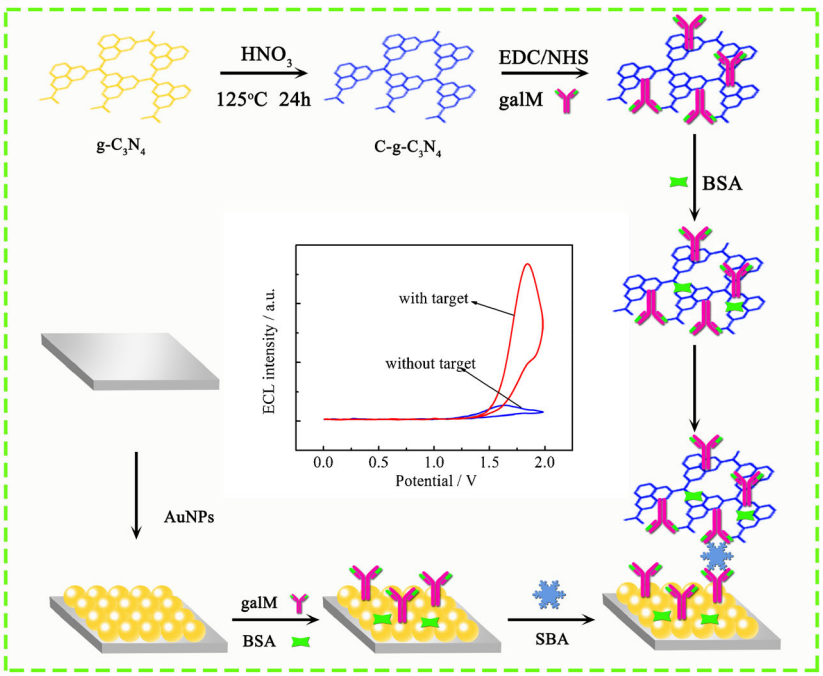

Scheme 1 The illustration of the preparation of the ECL biosensor

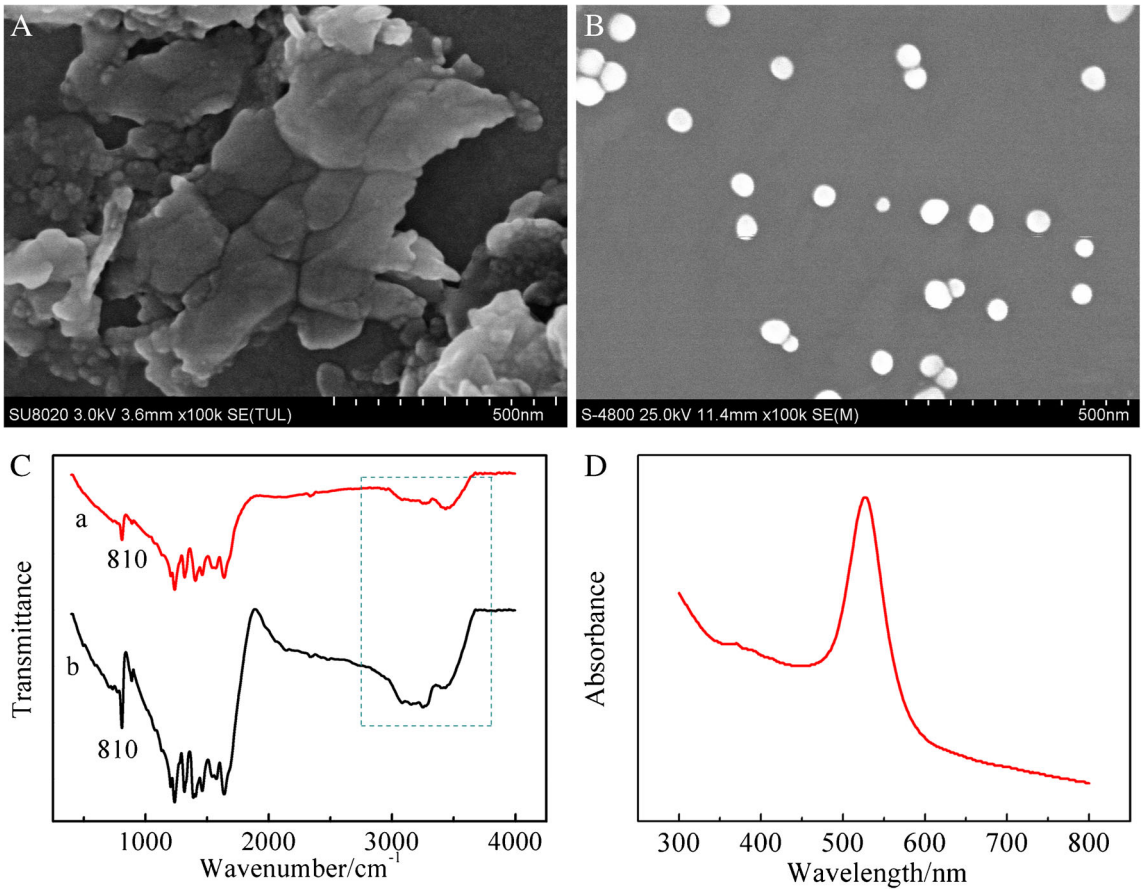

Fig. 1 SEM images of (**A**) C-g-C_3N_4 and (**B**) Au NPs. (**C**) The FT-IR spectra of (**a**) g-C_3N_4 and (**b**) C-g-C_3N_4. (**D**) UV-vis absorption spectra of Au NPs

C_3N_4. As seen, the obtained C-g-C_3N_4 was a sheet-like structure [24]. Figure 1B shows the SEM image of Au NPs and a relatively uniform size of 40–50 nm was observed. Figure 1D depicts the UV-vis absorption spectra of Au NPs and a distinct absorption peak at 530 nm was observed, indicating that Au NPs was successfully prepared.

The infrared spectroscopy (IR) of C-g-C_3N_4 was measured to prove that C-g-C_3N_4 was successfully prepared. As seen from Fig. 1C, a distinct absorption peak at 810 cm^{-1} derived from the vibration of the triazine ring was observed. The absorption peaks in the range of 850~1800 cm^{-1} corresponded to the vibration of the C − N(−C) − C or C − NH − C unit [25]. The absorption peaks in the range of 3000~3400 cm^{-1} were derived from the tensile mode of OH, COOH, and NH_2. Compared with curve a (g-C_3N_4), curve b (C-g-C_3N_4) exhibited stronger

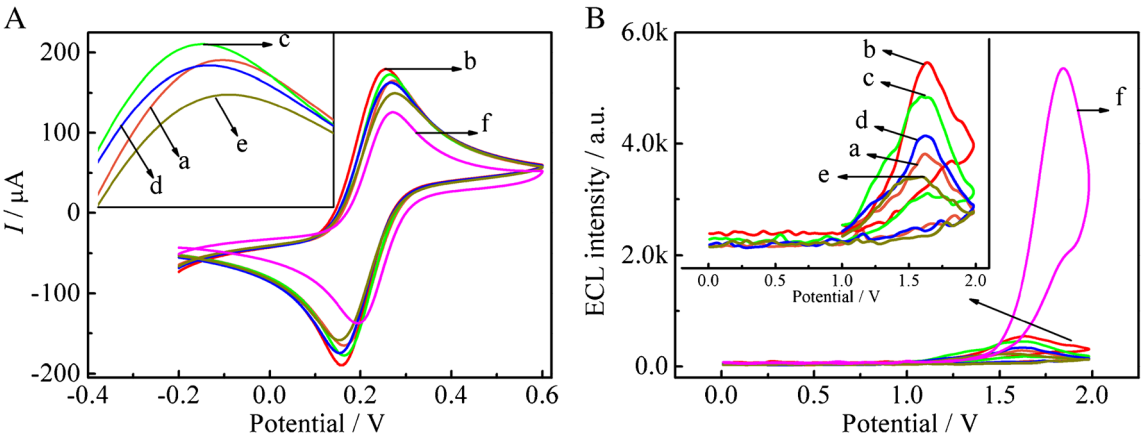

Fig. 2 (**A**) CV waves in 5.0 mM $K_3[Fe(CN)_6]/K_4[Fe(CN)_6]$ and (**B**) ECL responses at (**a**) bare GCE, (**b**) AuNPs/GCE, (**c**) galM/AuNPs/GCE, (**d**) BSA/galM/AuNPs/GCE, (**e**) SBA/BSA/galM/AuNPs/GCE, (**f**) C-g-C_3N_4-galM/SBA/BSA/galM/AuNPs/GCE

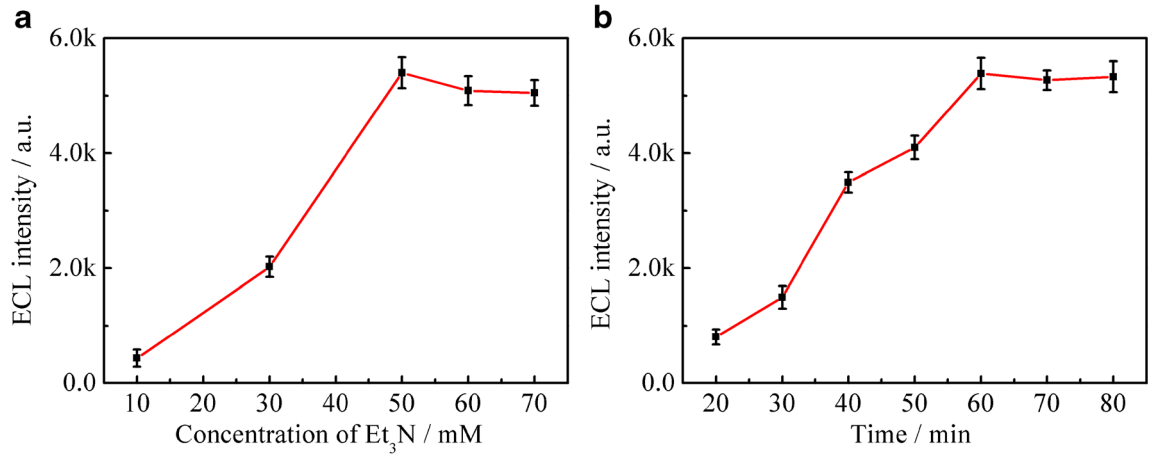

Fig. 3 **a** Effect of Et_3N concentration on the ECL responses in PBS (pH 7.4). **b** Effect of incubating time on the ECL responses in PBS (pH 7.4) containing 50 mM Et_3N

absorption in the region between 3000 and 3400 cm^{-1} [24], indicating that hydroxyl and carboxyl groups are formed during hydrothermal oxidation. The above results indicate that C-g-C_3N_4 was successfully prepared.

CV and ECL characterization of the biosensor

The CV detection was used to confirm the preparation process of the modified electrodes. The CV curves were recorded in 5 mM $[Fe(CN)_6]^{4-/3-}$ solution and the scan rate was 50 mV/s. Figure 2A presents corresponding CV curves. As seen, compared with the bare GCE (curve a), Au NPs modified GCE (curve b) displayed an increased redox wave due to the superior conductivity of Au NPs. With the incubation of galM on the electrode (curve c), the redox peak current decreased. After the electrode surface was blocked by BSA (curve d), a further decreased peak current was observed. When the SBA was captured onto the electrode surface, the redox peak current was further decreased (curve e). Decreased redox peak currents were described to the fact that galM, BSA SBA will impede the electron transfer. When C-g-C_3N_4-galM/BSA was incubated onto the electrode, the current was degraded due to the poor conductivity of C-g-C_3N_4-galM (curve f).

The ECL detection was used to further verify the preparation process of the biosensor. As shown in Fig. 2B, when the electrodes were modified step by step with Au NPs, galM, BSA, and SBA (curve b-e), the ECL signals are extremely weak because the C-g-C_3N_4 has not been modified onto the electrode. This weak luminescence intensity comes from $(^1O_2)_2$*. $(^1O_2)_2$* was produced by the reaction of $Et_3N^{\bullet+}$ and O_2^- [26]. As seen from curve f, after the C-g-C_3N_4-galM was captured onto the modified electrode, a greatly increased ECL intensity was observed due to the excellent ECL property of C-g-C_3N_4. The possible luminescence mechanism was as follows [27]:

$$C{-}g{-}C_3N_4{-}e{\rightarrow}C{-}g{-}C_3N_4^{\bullet+} \quad (1)$$

$$Et_3N{-}e{\rightarrow}Et_3N^{\bullet+} \quad (2)$$

$$Et_3N^{\bullet+}{-}H^+{\rightarrow}Et_3N^{\bullet} \quad (3)$$

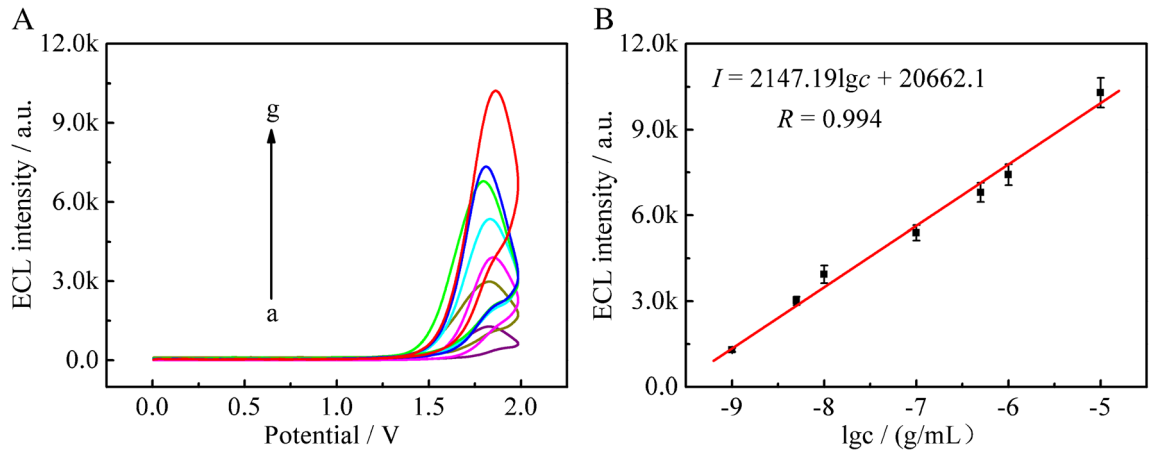

Fig. 4 **a** ECL response of the biosensor toward different concentrations of SBA: 1.0 ng/mL, 5.0 ng/mL, 10 ng/mL, 100 ng/mL, 500 ng/mL, 1.0 μg/mL, 10 μg/mL (from a to g) and **b** the relationship between ECL intensity and the logarithmic value of SBA concentration

Table 1 Comparison of reported methods for SBA determination

Method	Linear range (M)	Detection limit (M)	Reference
Voltammetry	1.0×10^{-9}–1.0×10^{-7}	2.0×10^{-10}	[28]
Voltammetry	3.3×10^{-9}–6.7×10^{-8}	1.6×10^{-9}	[29]
Voltammetry	2.5×10^{-12}–1.0×10^{-10}	8.0×10^{-13}	[16]
Electrochemiluminescence	8.3×10^{-12}–8.3×10^{-8}	2.8×10^{-12}	This work

$$C\text{–}g\text{–}C_3N_4^{\bullet+} + Et_3N^{\bullet} \rightarrow C\text{–}g\text{–}C_3N_4^{*} + Et_3Nox \quad (4)$$

$$C\text{–}g\text{–}C_3N_4^{*} \rightarrow C\text{–}g\text{–}C_3N_4 + h\nu \quad (5)$$

When applying voltage to the surface of the electrode, C-g-C_3N_4 could be oxidized and lose electron to form C-g-$C_3N_4^{\bullet+}$. Et_3N will also generate $Et_3N^{\bullet+}$ after being oxidized, and then $Et_3N^{\bullet}$ can be obtained by releasing a proton from $Et_3N^{\bullet+}$. Subsequently, the resulting $Et_3N^{\bullet}$ can react with C-g-$C_3N_4^{\bullet+}$ via electron transfer to form C-g-C_3N_4*, which acted as an emitting species to lead to an intense emission.

Optimization of experimental conditions

The concentration of Et_3N was optimized using the biosensor incubated with 100 ng/mL SBA. As observed in Fig. 3a, the ECL intensity consecutively increased with the increase of Et_3N concentration from 10 to 50 mM. When Et_3N concentration was higher than 50 mM, the ECL signal did not exhibit a significant enhancement. Therefore, 50 mM was chosen for the optimum concentration of Et_3N.

The incubation time of SBA was optimized and Fig. 3b shows the corresponding results. With the increase of the incubation time of SBA from 20 to 60 min, the ECL response increased accordingly and a plateau was observed after 60 min. Therefore, 60 min was chosen as the incubation time of SBA in this experiment.

ECL response for SBA detection

The ECL response of the biosensor toward SBA was detected under the optimal conditions. As seen in Fig. 4a, with the increase in SBA concentration, the ECL signal

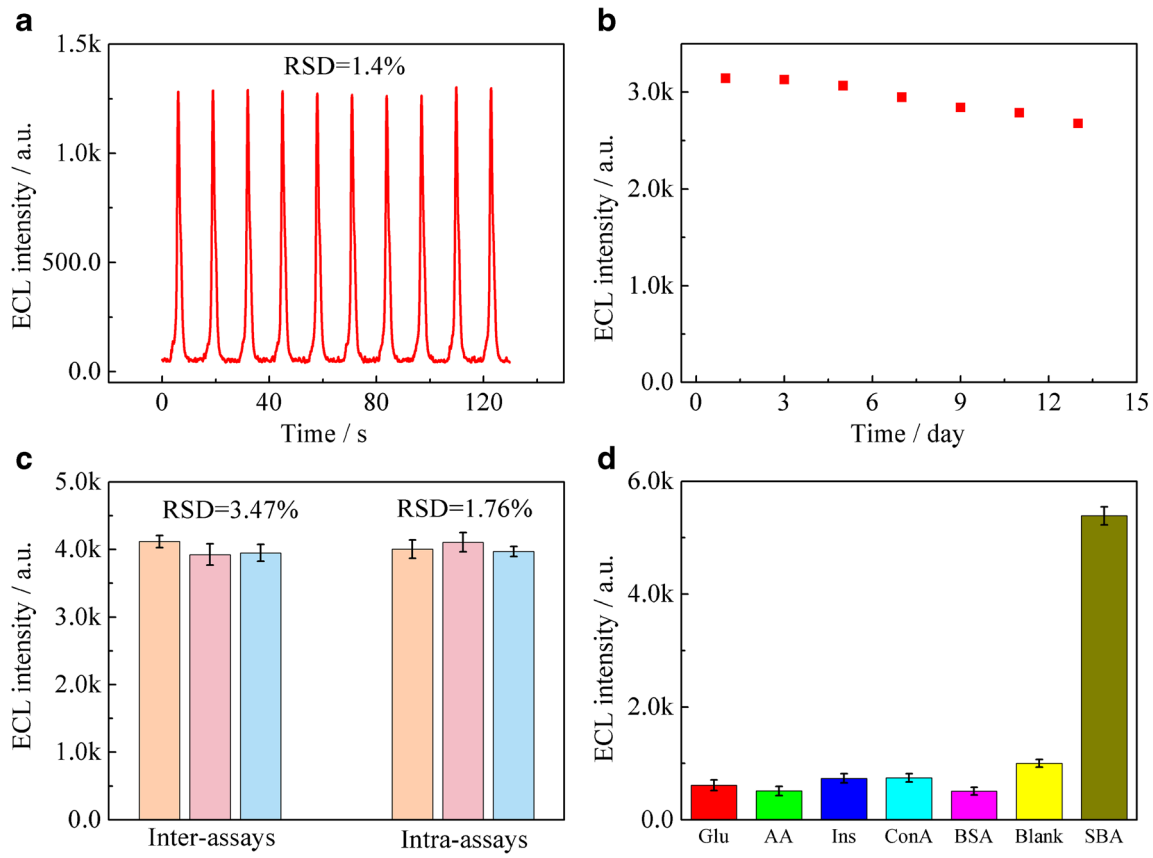

Fig. 5 **a** The stability of the biosensor with 1 ng/mL SBA. **b** The time-dependent stability of the biosensor with 5 ng/mL SBA. **c** Reproducibility of the proposed biosensor with 10 ng/mL SBA. **d** Specificity of the proposed biosensor toward different interfering substances

Table 2 Recoveries of SBA by the biosensor in human serum

Samples	Added (ng/mL)	Found[a] (ng/mL)	Recovery (%)
1	1.000	0.9958 ± 0.053	99.58
2	100.0	100.1 ± 3.17	100.1
3	1000	933.3 ± 50.9	93.33

[a] Average of three determination ± SD, $n = 3$

increased gradually. A good linear relationship was observed between the ECL intensity and the logarithm of SBA concentration (Fig. 4b). The regression equation was expressed as $I = 2147.19\lg c + 20{,}662.1$ and the correlation coefficient R was 0.994. The linear range of the prepared biosensor was from 1 ng/mL to 10 μg/mL and the detection limit is 0.33 ng/mL. Additionally, a comparison of the analytical performance between our proposed biosensor and previously reported SBA detection methods was performed. As seen from Table 1, the proposed biosensor exhibited a wide linear range and a lower detection limit than other approaches.

Stability, reproducibility, and selectivity of the biosensor

The stability of the biosensor was investigated from the following two aspects. On the one hand, the biosensor incubated 1 ng/mL SBA was continuously scanned for ten cycles and the results are shown in Fig. 5a. The relative standard deviation (RSD) of ECL signals is 1.4%. On the other hand, the long-term stability of the biosensor incubated with 5 ng/mL SBA was tested. The ECL signal of the biosensor was detected every 2 days. As shown in Fig. 5b, 13 days later, the ECL signal decreased 14.7%, indicating an acceptable stability of the biosensor.

The inter- and intra-assays were performed to investigate the reproducibility of the biosensor. Intra-assays were performed using three biosensors prepared in the same batch and inter-assays were performed using three biosensors prepared in different batches, and the results are shown in Fig. 5c. The RSD of inter- and intra-assays was 3.47% and 1.76%, respectively, indicating a good reproducibility of the constructed biosensor.

The selectivity of the biosensor was investigated, and glucose (Glu), ascorbic acid (AA), insulinum (Ins), Concanavalin A (Con A), and bovine serum albumin (BSA) were selected as possible interfering agents. As described in Fig. 5d, the ECL intensity was significantly increased in the presence of SBA, while Glu, AA, Ins, Con A, and BSA did not lead an obvious increased ECL response when compared to the blank solution, indicating a good anti-interference capability of the biosensor.

Application of the biosensor

The practical application of the biosensor was investigated using standard addition method. The recovery of SBA in human serum samples was detected and the results are shown in Table 2. The recoveries of SBA were between 93.33 and 100.1%, indicating that the proposed sensor may be used in practical detection.

Conclusions

In this work, C-g-C_3N_4 with abundant carboxyl groups not only acted as an excellent signal probe but also served as an ideal immobilization matrix to achieve a high loading of recognition element galM of SBA. The combination of the character as an ideal immobilization matrix and the excellent ECL performance of C-g-C_3N_4 endows the biosensor excellent analytical performance, including a low detection limit and a wide linear range, and a good stability, selectivity, and reproducibility for SBA detection. This strategy provides an appealing platform for the ECL detection of SBA.

Funding information This work was supported by the National Natural Science Foundation of China (21775122, 21775123, 51473136, 21575116, 21705115), Natural Science Foundation of Chongqing City (cstc2018jcyjAX0693) China, Natural Science Foundation of Jiangsu Province of China (BK20170378), Natural Science Research Foundation of Jiangsu Higher Education Institutions (17KJB150036), and Key Laboratory of Sensor Analysis of Tumor Marker, Ministry of Education, Qingdao University of Science and Technology (SATM201604).

Compliance with ethical standards

Conflict of interest The authors declare that they have no conflict interest.

References

1. Liu ZY, Qi WJ, Xu GB. Recent advances in electrochemiluminescence. Chem Soc Rev. 2015;44:3117–42.
2. Spehar-Délèze AM, Julich S, Gransee R, Tomaso H, Dulay SB, O'Sullivan CK. Electrochemiluminescence (ECL) immunosensor for detection of Francisella tularensis on screen-printed gold electrode array. Anal Bioanal Chem. 2016;408:7147–53.
3. Hao N, Wang K. Recent development of electrochemiluminescence sensors for food analysis. Anal Bioanal Chem. 2016;408:7035–48.
4. Nasiri Khonsari YS, Sun SG. Recent trends in electrochemiluminescence aptasensors and their applications. Chem Commun. 2017;53:9042–54.
5. Zhang P, Jiang J, Yuan R, Zhuo Y, Chai YQ. Highly ordered and field-free 3D DNA nanostructure: the next generation of DNA nanomachine for rapid single-step sensing. J Am Chem Soc. 2018;140:9361–4.

6. Yang X, Yu YQ, Peng LZ, Lei YM, Chai YQ, Yuan R, et al. Strong electrochemiluminescence from MOF accelerator enriched quantum dots for enhanced sensing of trace cTnI. Anal Chem. 2018;90:3995–4002.
7. Li ZY, Lin ZF, Wu XY, Chen HT, Chai YQ, Yuan R. Highly efficient electrochemiluminescence resonance energy transfer system in one nanostructure: its application for ultrasensitive detection of microRNA in cancer cells. Anal Chem. 2017;89:6029–35.
8. Xiong MY, Rong QM, Meng HM, Zhang XB. Two-dimensional graphitic carbon nitride nanosheets for biosensing applications. Biosens Bioelectron. 2017;89:212–23.
9. Du XJ, Jiang D, Dai LM, Zhu WR, Yang XD, Hao N, et al. Oxygen vacancy engineering in europia clusters/graphite-like carbon nitride nanostructures induced signal amplification for highly efficient electrochemiluminesce aptasensing. Anal Chem. 2018;90:3615–20.
10. Chen LC, Zeng XT, Si P, Chen YM, Chi YW, Kim DH, et al. Gold nanoparticle-graphite-like C_3N_4 nanosheet nanohybrids used for electrochemiluminescent immunosensor. Anal Chem. 2014;86:4188–95.
11. Zhan TR, Tan ZW, Wang XJ, Hou WG. Hemoglobin immobilized in g-C_3N_4 nanoparticle decorated 3D graphene-LDH network: direct electrochemistry and electrocatalysis to trichloroacetic acid. Sensors Actuators B Chem. 2018;255:149–58.
12. Sattsangi PD, Sattsangi S, Grossman HH. Isolation of soybean agglutinin (SBA) from soy meal. J Chem Educ. 1982;59:977–9.
13. Etzler ME. Plant lectins: molecular and biological aspects. Ann Rev Plant Physiol. 1985;36:209–34.
14. Pan L, Farouk MH, Qin GX, Zhao Y, Bao N. The influences of soybean agglutinin and functional oligosaccharides on the intestinal tract of monogastric animals. Int J Mol Sci. 2018;19:554.
15. Chen YL, Ding L, Liu TT, Ju HX. Arrayed profiling of multiple glycans on whole living cell surfaces. Anal Chem. 2013;85:11153–8.
16. Sugawara K, Kadoya T, Kuramitz H. Magnetic beads modified with an electron-transfer carbohydratemimetic peptide for sensing of a galactose dependent protein. Anal Chim Acta. 2018;1001:158–67.
17. Rizzi C, Galeoto L, Zoccatelli G, Vincenzi S, Chignola R, Peruffo ADB. Active soybean lectin in foods: quantitative determination by ELISA using immobilised asialofetuin. Food Res Int. 2003;36:815–21.
18. Fan Y, Tan XR, Ou X, Chen SH, Wei SP. An ultrasensitive electrochemiluminescence biosensor for the detection of concanavalin A based on Au nanoparticles-thiosemicarbazide functionalized PtNi nanocubes as signal enhancer. Biosens Bioelectron. 2017;87:802–6.
19. Li XJ, Wang YG, Shi L, Ma HM, Zhang Y, Du B, et al. A novel ECL biosensor for the detection of concanavalin A based on glucose functionalized $NiCo_2S_4$ nanoparticles-grown on carboxylic graphene as quenching probe. Biosens Bioelectron. 2017;96:113–20.
20. Wang BX, Zhong X, Chai YQ, Yuan R. An ECL biosensor for sensitive detection of concanavalin A based on the ECL quenching of Ru complex by MoS_2 nanoflower. Sensors Actuators B Chem. 2017;245:247–55.
21. Chen SH, Fan Y, Zhang C, He YY, Wei SP. Quenched solid-state electrochemiluminescence of gold nanoclusters and the application in the ultrasensitive detection of concanavalin A. Electrochim Acta. 2017;228:195–202.
22. Wang HY, Qi CL, He WH, Wang MH, Jiang WJ, Yin HS. A sensitive photoelectrochemical immunoassay of N^6 methyladenosine based on dual-signal amplification strategy: Ru doped in SiO_2 nanosphere and carboxylated g-C_3N_4. Biosens Bioelectron. 2018;99:281–8.
23. Liu XL, Liang S, Nan F, Yang ZJ, Yu XF, Zhou L, et al. Solution-dispersible Au nanocube dimers with greatly enhanced two-photon luminescence and SERS. Nanoscale. 2013;5:5368–74.
24. Shiravand G, Badiei A, Ziarani GM. Carboxyl-rich g-C_3N_4 nanoparticles: synthesis, characterization and their application for selective fluorescence sensing of Hg^{2+} and Fe^{3+} in aqueous media. Sensors Actuators B Chem. 2017;242:244–52.
25. Deng SY, Yuan PX, Ji XB, Shan D, Zhang XJ. Carbon nitride nanosheet-supported porphyrin: a new biomimetic catalyst for highly efficient bioanalysis. ACS Appl Mater Interfaces. 2015;7:543–52.
26. Kumar SS, Bard AJ. Background emission of electrogenerated chemiluminescence during oxidation of tri-n-propylamine from the dimeric $^1\Delta_g$ state of O_2. Anal Chem. 2013;85:292–5.
27. Wang BX, Wang HJ, Zhong X, Chai YQ, Chen SH, Yuan R. A highly sensitive electrochemiluminescence biosensor for the detection of organophosphate pesticides based on cyclodextrin functionalized graphitic carbon nitride and enzyme inhibition. Chem Commun. 2016;52:5049–52.
28. Kuramitz H, Mawatari Y, Ikeuchi M, Kutomi O, Hata N, Taguchi S, et al. Multiplexed assay for proteins based on sequestration electrochemistry using the protein binding electroactive magnetic microbeads. Anal Sci. 2012;28:77–81.
29. Sugawara K, Kuramitz H, Kaneko T, Hoshi S, Akatsuka K, Tanaka S. Voltammetric detection of lectin using sugar labeled with electroactive substance. Anal Sci. 2001;17:21–5.